

KEK-TH-477
YUMS-96-27
SNUTP-96-110
 (January 6, 2018)

Virtual SUSY Threshold Effects and CDF large E_T Anomaly

C.S. Kim^{1,2*} and S. Alam^{2†}

1: *Department of Physics, Yonsei University, Seoul 120-749, Korea*

2: *Theory Group, KEK, Tsukuba, Ibaraki 305, Japan*

Abstract

Recent CDF data of the inclusive jet cross section shows threshold-like structured deviation, around transverse momentum $E_T(j) \approx 200 \sim 350$ GeV. If this data is real, not just some statistical fluctuation, is it possible to interpret the anomaly in terms of virtual SUSY effects? The purpose of this note is to address this question. However, we find that virtual SUSY loop interference effects [near the threshold] are too small to explain the CDF data. Our main conclusion seems to be on the right track if we assume that the recent global analysis of improved parton distributions by Lai *et al.* is correct.

*cskim@kek.vax.kek.jp, kim@cskim.yonsei.ac.kr

†sher@theory.kek.jp

I. INTRODUCTION

The CDF [1] and D0 [2] collaborations at Tevatron Collider have recently reported data for the inclusive jet cross section in $p\bar{p}$ collisions at $\sqrt{s} = 1800$ GeV. Let us recapitulate some particulars of this data [we concentrate mainly on the CDF data].

- The CDF measurement is based on a data sample of 19.5 pb^{-1} collected in 1992-93 with the CDF detector at the Tevatron collider. Jets were reconstructed using a cone algorithm.
- Cosmic rays and accelerator loss backgrounds were removed with cuts on event energy timing and on missing transverse energy. The remaining backgrounds are claimed to be less 0.5% in any E_T bin.
- The measurements have been reported over a wide range of transverse energy, $15 \text{ GeV} \leq E_T \leq 440 \text{ GeV}$, and around the central pseudorapidity region $0.1 \leq |\eta| \leq 0.7$. The smallest distance probed is on the order of 10^{-19} m .
- After accounting for uncertainties the corrected experimental cross section, when compared to the Next-to-leading [NLO] QCD predictions using MRSD0' parton distribution function [PDF's], is significantly higher than the NLO prediction for $E_T > 200 \text{ GeV}$. For E_T below 200 GeV the agreement between the CDF and the NLO QCD cross section is excellent, while the D0 results are higher than the NLO PQCD predictions within the statistical uncertainties.
- CDF collaboration have compared their data with other PDF's and a model about presence of quark substructure. This will be discussed later.

There are basically two logical possibilities for explanations of the CDF data on inclusive jet production cross sections: (i) the parton distribution functions determined at low Q^2 region may not be accurate enough to be applicable to the high E_T region with $E_T > 200$ GeV, or (ii) there are some new physics around the electroweak scale. We give a brief review of these two possibilities in the following.

Let us first consider the first possibility. According to the CDF collaboration [1] “the excess of data over theory at high E_T remains for CTEQ2M, CTEQ2ML, GRV94, MRSA’, and MRSG parton distribution”. The variations in QCD predictions represented a survey of then-available distributions. They do not represent the uncertainties associated with data used in deriving the PDF’s. Inclusion of these new data in a global fit with those from other experiments may yield a consistent set of PDF’s which will accommodate the high- E_T excess within the scope of QCD. Glover *et al.*, [3] conclude that “it is unlikely that the difference between the CDF inclusive jet cross section data and standard NLO QCD prediction can be attributed to a deficiency in our knowledge of parton distributions”. More precisely Glover *et al.* [3] find from their global analysis that it is impossible to fit both the CDF data for $E_T > 200$ GeV and Deep Inelastic Scattering [DIS] data for $x > 0.3$. However, as noted in [8] the interpretation of large E_T jet cross sections inherits uncertainties from the non-perturbative parton distribution and fragmentation functions. It has recently been reported [4] that the apparent discrepancy between CDF data and theory may be explained by the uncertainties resulting from the non-perturbative parton distribution, in particular in the gluon distribution at large x . These authors have also performed NLO QCD global analysis including the CDF data and conclude that high E_T can be explained in terms of a modified gluon PDF. However, we note that Lai *et al.* [4] use more parameters to describe the input gluon distribution than is usually done, whereas Glover *et al.* [3] assume that the gluon distribution has a canonical behavior [i.e. goes as $(1 - x)^n$] at large x .

It is also tempting to look for a possible explanation for the CDF data in terms of new physics. The CDF group [1] have reported on a model of presence of quark substructure [5]. They have compared their data to leading order QCD calculation including compositeness and have used MRSD0' parton distribution. They find a good agreement between data and the compositeness model, for $E_T > 200$ GeV, for a substructure scale of $\Lambda_C = 1.6$ TeV.

Yet another possibility is that jet measurements at hadron colliders may be sensitive to quantum corrections due to virtual SUSY particles [6–9]. The purpose of this note is to concentrate on this scenario. The layout and of this paper is as follows. In next section we discuss our calculation of the SUSY virtual threshold effects. The final section contains discussions and conclusions of our numerical results.

II. VIRTUAL SUSY THRESHOLD EFFECTS

We consider the SUSY one loop corrections to the process $d\sigma(p\bar{p} \rightarrow 2 \text{ jets})$. As is well-known, the 2 jets production cross section in proton anti-proton collisions is found by weighing the expressions for differential cross section of the subprocess, $d\hat{\sigma}_{ij} \equiv d\hat{\sigma}(ij \rightarrow 2 \text{ final partons})$, by the parton distribution functions, and integrating over the parton variables, i.e.

$$d\sigma(p\bar{p} \rightarrow 2 \text{ jets}) = \sum_{i,j} \int_0^1 dx_1 \int_0^1 dx_2 [f_{i/p}(x_1, Q^2) f_{j/\bar{p}}(x_2, Q^2)] d\hat{\sigma}_{ij}(\alpha_s, \hat{s}, \hat{t}, \hat{u}). \quad (1)$$

Here $d\hat{\sigma}_{ij}$ represents the subprocess cross section at c.m. energy square of $\hat{s} = x_1 x_2 s$, where \sqrt{s} is the c.m. energy of the $p\bar{p}$ system. It is well-known that SUSY particles [gluinos, squarks] decrease or slow down the rate of fall of $\alpha_s(\mu)$ for large scale μ . “Large” means far above the threshold. At the one loop level the evolution equation for $\alpha_s(\mu)$ can be written as

$$\frac{d}{d \ln \mu} \alpha_s(\mu) = -\frac{b_3}{2\pi} \alpha_s^2(\mu) . \quad (2)$$

In the SM, b_3 is given by

$$b_3 = 11 - \frac{2}{3} n_f , \quad (3)$$

whereas in MSSM model one has

$$b_3 = 11 - \frac{2}{3} n_f - 2 - \frac{1}{3} \tilde{n}_f , \quad (4)$$

where n_f [\tilde{n}_f] is the number of quark [squark] flavors that are active. The contribution ‘ -2 ’ is the gluino contribution [it is assumed that the gluino is active in this case].

With this in mind, we can see that the SUSY corrections to Eq. (1) can be broken into three parts, namely (a): SUSY corrections to the PDF, (b): SUSY corrections to the running of α_s , (c): parton-level SUSY loop corrections to $d\hat{\sigma}_{ij}$, excluding the corrections already included in (b) [i.e. the running of α_s]. And finally we have to (d): combine those three part, as in Eq. (1), by convoluting with PDF to get hadron-level SUSY interference effects. In this note we consider all these four parts [i.e. (a),(b),(c),(d)]. Previous works on SUSY corrections [6–8] have considered only part of them: In Ref. [6] only the issue of the effect of high-mass thresholds due to gluinos, squarks and other new heavy quarks on the evolution of α_s was considered [i.e. (b)]. The corrections to α_s were found to be appreciable, this in turn means a significant increase in the transverse momentum dependence of jet production at the Tevatron. However, as noted in Ref. [7], these authors [6] do not include the effect of $q\tilde{q}\tilde{g}$ Yukawa interactions, and hence one cannot take their estimates for the superpartners of ordinary matter as final. In Ref. [7] the effect of Yukawa couplings was included, and found that the CDF data cannot be explained by a mass threshold effect in the MSSM, as the calculated result is not only small but of the wrong sign, considered at the parton level below the threshold energy scale [i.e. (b),(c)]. In a similar but more detailed analysis, the

authors of Ref. [8], working in the context of MSSM, consider at around the threshold energy scale the virtual one-loop corrections to the parton-level subprocesses $q\bar{q} \rightarrow q\bar{q}$, $q\bar{q} \rightarrow q'\bar{q}'$, $qq' \rightarrow qq'$, $q\bar{q} \rightarrow gg$ and $qg \rightarrow qg$, which are expected to dominate the large E_T cross sections at the Tevatron energy [i.e. (b),(c)].

The purpose of this note is to give our results of incorporating the one-loop radiative corrections into the running of α_s , the dressing-up of the parton distribution functions, and finally convoluting the relevant subprocess cross sections with the SUSY dressed-up PDF's [i.e. (a),(b),(c),(d)]. In the hadron colliders, like the Tevatron, what is measured is $p\bar{p}$ cross section, and not the individual subprocesses cross sections. So in order to determine the effect of subprocesses on the E_T cross section one must perform a convolution of the cross section of each subprocess with the corresponding PDF's [i.e. (d)]. We find that in the process of convolution with the PDF's, the "dips and peaks" in the various subprocesses [8] are much reduced.

We note that, also as pointed out in [8], one should take into account sparticles effects on the parton structure functions at energies **sufficiently far above** the threshold, and can ignore this effect around the threshold region [i.e. (a)]. We test the validity of this statement and find it to be true from our numerical work, as will be shown in Fig. 2. We have considered the combined evolution equations for α_s , q_v

$$\frac{d}{d \ln Q^2} \alpha_s(Q^2) = -\frac{b_3}{4\pi} \alpha_s^2(Q^2) , \quad (5)$$

$$\frac{d}{d \ln Q^2} q^{NS}(x, Q^2) = \frac{\alpha_s(Q^2)}{2\pi} P_0^{NS} \otimes q^{NS}(x, Q^2) . \quad (6)$$

The second equation becomes, with the definition of $p^{NS} = xq^{NS}$,

$$\begin{aligned} \frac{d}{d \ln Q^2} [p^{NS}(x, Q^2)] &= \frac{2\alpha_s(Q^2)}{3\pi} \int_x^1 \frac{dz}{1-z} [(1+z^2)[p^{NS}(x/z, Q^2)] - 2p^{NS}(Q^2, x)] \\ &\quad + \frac{\alpha_s(Q^2)}{\pi} [1 + \frac{4}{3} \ln(1-x)] p^{NS}(x, Q^2) . \end{aligned} \quad (7)$$

The increase of $\alpha_s(Q^2)$ results in the decrease of the PDF compared to the SM when we make the evolution. The qualitative reason is rather simple: stronger $\alpha_s(Q^2)$ as Q^2 increases imply that the gluon radiation from the initial quarks are enhanced, and the PDF evolution yields the larger gluon or sea-quark densities at the smaller x region, and therefore the valence quark distribution $q_v(x, Q^2)$ decreases at large x , as $\alpha_s(Q^2)$ increases, and vice versa. We recall that for large x the valence contribution dominates (e.g. $q_v \cdot q_v : q_v \cdot g : g \cdot g \sim 0.65 : 0.3 : 0.05$ at $x \sim 0.3$ at Tevatron energies), we ignored the SUSY evolution of sea-quark or gluon for large E_T of CDF. It turns out, as shown in Fig. 2 and claimed in Ref. [8], the PDF with sparticle effects at around the threshold region deviates much less than 0.1% from its SM predictions, which justifies our assumption. And we can even totally ignore the SUSY corrections to PDF [i.e. (a)] all together for investigations below or around the threshold region.

III. NUMERICAL RESULTS AND CONCLUSIONS

For our numerical calculation, we implement various lower bounds on squarks and gluinos depending on parameters in the MSSM. For example, D0 group [10] searched for the events with large missing E_T with three or more jets, observed no such events above the level expected in the SM. This puts some limits on the squark and gluino masses assuming the short-lived gluinos:

$$m_{\tilde{g}} > 144 \text{ GeV} \quad \text{for} \quad m_{\tilde{q}} = \infty , \quad (8)$$

$$\text{or} \quad m_{\tilde{g}} = m_{\tilde{q}} > 212 \text{ GeV} . \quad (9)$$

CDF group is currently analyzing their data, with their preliminary data being similar to the D0 results with slight increase in sparticles' mass bound. In the subsequent numerical

analysis, we choose three sets of $(m_{\tilde{g}}, m_{\tilde{q}})$, which we shall refer to as Case I, II and III, respectively,

$$(m_{\tilde{g}}, m_{\tilde{q}}) = (220 \text{ GeV}, 220 \text{ GeV}), \quad (150 \text{ GeV}, \infty), \quad (150 \text{ GeV}, 150 \text{ GeV}) . \quad (10)$$

The Case III is only of academic interest if the limit given in Eq. (9) is valid in reality.

We turn now to our numerical result. The solid curve in Fig. 1 represents the one-loop evolution of $\alpha_s(\mu)$ versus the renormalization scale μ for the SM, assuming a top-quark mass of 175 GeV, and $\Lambda_{QCD} = 0.2$ GeV. The long-dashed curve represents the results for the MSSM with the five squarks and gluinos being degenerate with a common mass of 220 GeV [we shall refer to this as Case I]. As can be seen from Fig. 1, Case I starts to deviate from the SM results at $\mu = 440$ GeV, as expected. The deviation in the value of α_s away from the SM is maximum [for our range of μ] at $\mu = 700$ GeV and roughly on the order of 5%. This value is to be compared to the 12% reported in [6]. The dotted curve in Fig. 1 describes our result for the MSSM with gluino mass of 150 GeV, and the squarks are assumed to be decoupled, we shall refer to this as Case II. Case II starts to be different from the SM at $\mu = 300$ GeV. The maximum deviation for Case II occurs at around 700 GeV, where it also approaches the curve for Case I.

The deviation from the SM of the one-loop evolution for the parton distribution function $[(\frac{\text{MSSM-SM}}{\text{SM}})u_v(Q)]$ versus the factorization scale Q for Cases I and II are shown in Fig. 2. Case I deviates from the SM at $Q = 440$ GeV attaining a maximum change of -0.05% at 700 GeV. The magnitude of deviation is much smaller compared to the results of Case I displayed in Fig. 1. The sign of corrections is also opposite to those for Case I in Fig. 1. This indicates as that α_s increases [as for *e.g.* it does for MSSM] $u_v(Q)$ decreases. This is natural to expect since for larger α_s there is more probability of gluon radiation, which in turn implies larger gluon and sea densities at small x , which eat away at the u_v contribution

thus resulting in a reduction in u_v . Turning to Case II, we see from Fig. 2 that it deviates from the SM at $Q = 300$ GeV, reaching a maximum value of only -0.1% at 700 GeV.

Fig. 3 exhibits our results for $[(\frac{\text{MSSM-SM}}{\text{SM}}) \frac{d\sigma}{dp_{T_j}}]$ versus p_{T_j} for both Cases I and III [Case III refers the MSSM with the five squarks and gluinos being degenerate with a common mass of 150 GeV, *i.e.* the last set in Eq. (10)]. A rapidity cut of 0.7 is used $[\lvert\eta\rvert < 0.7]$. A maximum difference of -1% from the SM is found for the both Cases. The question that naturally arises is, that why the “dips and peaks” [which are at the level of 5%–6% [8]] at the parton level, are reduced. There are two factors contributing to the reduction in the “dips and peaks” in the process of going from the parton to the process level. Part of this reduction comes from the process of convolution of the various subprocesses with PDF’s [as already remarked to in the previous section]. The other piece of this reduction in “dips and peaks” by going from subprocess to process level is due to t-channel “dilution” effect. This can be shown by simply not including the t-channel subprocesses’ contribution. When this is done [see Fig. 4a and 4b] reduction in the “peaks and dips” is not so large.

In Fig. 4(a) we exhibit our results for $[(\frac{\text{MSSM-SM}}{\text{SM}}) \frac{d\sigma}{dp_{T_j}}]$ versus p_{T_j} for both Cases I and III, but this time only including the subprocesses $q\bar{q} \rightarrow q'\bar{q}'$ and $q\bar{q} \rightarrow gg$. These two are the subprocesses with the prominent threshold structures from vacuum polarization interferences through s -channel exchange diagrams. A rapidity cut of 0.7 is used $[\lvert\eta\rvert < 0.7]$. The deviation from the SM for Case I varies between 2% to -4% , whereas as in Case II the variation is similar size to Case I at different energy scales related to the SUSY threshold effects. In Fig. 4(b) we exhibit our results for $[(\frac{\text{MSSM-SM}}{\text{SM}}) \frac{d\sigma}{dM_{jj}}]$ versus M_{jj} for both the Cases I and III, including the subprocesses $q\bar{q} \rightarrow q'\bar{q}'$ and $q\bar{q} \rightarrow gg$. The percentage variation is almost the same as in Fig. 4(a).

Near the virtual (or direct) SUSY threshold, the Coulomb interactions between the gluinos [or squarks] with a very small velocity $v = \sqrt{1 - 4m_g^2/Q^2}$ make the QCD effects

depending on the parameter α_s/v , rather than on α_s . The result of summing up the Coulomb exchanges reduces to multiplying the Coulomb factor α_s/v [11], which gives a wide resonance structure around $Q \approx 2m_{\tilde{g}}$ for the short-lived gluino pairs. If the life time of gluino is long enough, then narrow bound states of gluino pair may appear near the threshold region. Since the properties on gluino pair bound states are not known and largely model dependent, we can guess only qualitative nature of the threshold region, $Q \approx 2m_{\tilde{g}}$ (or $Q \approx 2m_{\tilde{q}}$), as shown in Fig. 3 and 4.

In summary, in the MSSM the E_T distributions does not differ very much from those of the SM except for the possible threshold effects ($\sim 1\%$) through loop corrections. In actual experiments, the jet resolution will in general smear out any narrow resonance structures (which may be the case for the long-lived gluinos), leading to broad resonance structure, and therefore it looks impossible to detect SUSY particles through this kind of indirect virtual threshold effect. As is previously explained, it has been reported [4] that the apparent discrepancy between CDF data and theory may be explained by the uncertainties resulting from the non-perturbative parton distribution, in particular in the gluon distribution. Our main conclusion seems to be on the right track in view of this global analysis of parton distribution function.

ACKNOWLEDGEMENTS

The authors would like to thank E.L. Berger, M. Drees, P. Ko, Jake Lee and J.W. Qui for useful suggestions and helpful comments. The work of CSK was supported in part by the KOSEF, Project No. 951-0207-008-2, in part by CTP of SNU, in part by the BSRI Program, Project No. BSRI-97-2425, and in part by the COE Fellowship from Japanese Ministry of Education, Science and Culture. The work of SA is supported by COE fellowship of the Japanese Ministry of Education, Science and Culture.

REFERENCES

- [1] CDF Collaboration: F. Abe *et al.*, Phys. Rev. Lett. **77** (1996) 438.
- [2] D0 Collaboration: G. Blazey, talk given at Recontre de Moriond, (March 1996).
- [3] E.W.N. Glover *et al.*, Phys. Lett. **B381** (1996) 353.
- [4] H.L. Lai *et al.*, hep-ph/9606399.
- [5] E. Eichten *et al.*, Phys. Rev. Lett. **50** (1983) 811.
- [6] V. Barger *et al.*, Phys. Lett. **B383** (1996) 178.
- [7] P. Kraus and F. Wilczek, Phys. Lett. **B382** (1996) 262.
- [8] J. Ellis and D. Ross, Phys. Lett. **B383** (1996) 187.
- [9] S. Alam *et al.*, Phys. Rev. **D55** (1997) 1.
- [10] D0 Collaboration: S. Abachi *et al.*, Phys. Rev. Lett. **75** (1995) 618.
- [11] V.S. Fadin *et al.*, Yad. Fiz. **48** (1988) 309.

FIGURES

Fig. 1 The one-loop evolution of $\alpha_s(\mu)$ versus μ is given for SM [solid line] and SUSY cases.

Fig. 2 Percentage deviation from the SM due to SUSY contribution of PDF of the valence quark versus factorization scale Q for typical momentum fraction $x = 0.3$.

Fig. 3 Deviation from the SM due to SUSY contribution to $\frac{d\sigma}{dp_{Tj}}$ versus p_{Tj} .

Fig. 4a Deviation from the SM due to SUSY contribution to $\frac{d\sigma}{dp_{Tj}}$ versus p_{Tj} , when only the subprocesses $q\bar{q} \rightarrow q'\bar{q}'$, and $q\bar{q} \rightarrow gg$ are included.

Fig. 4b Deviation from the SM due to SUSY contribution to $\frac{d\sigma}{dM_{jj}}$ versus M_{jj} , when only the subprocesses $q\bar{q} \rightarrow q'\bar{q}'$, and $q\bar{q} \rightarrow gg$ are included.

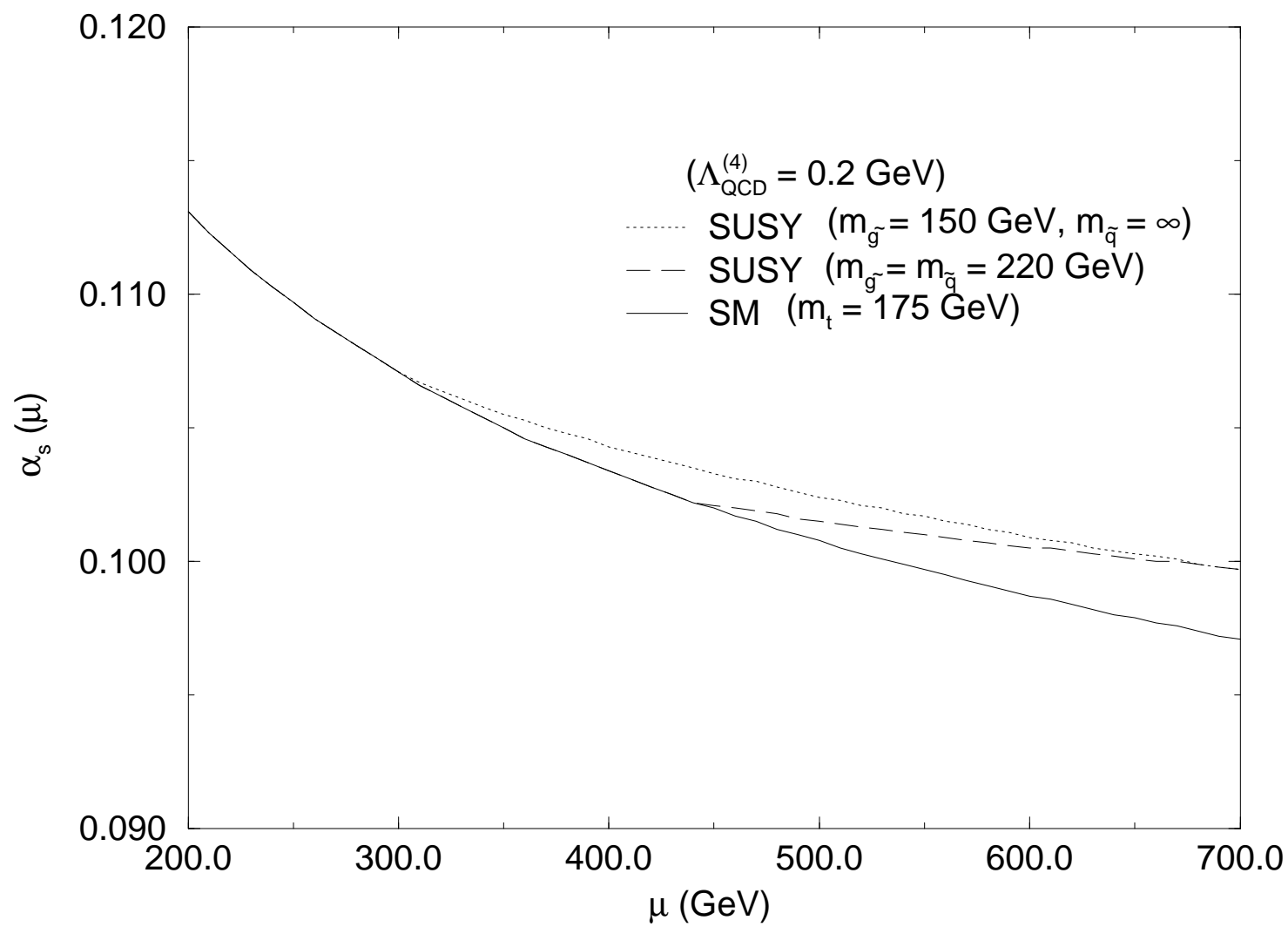


Fig. 1

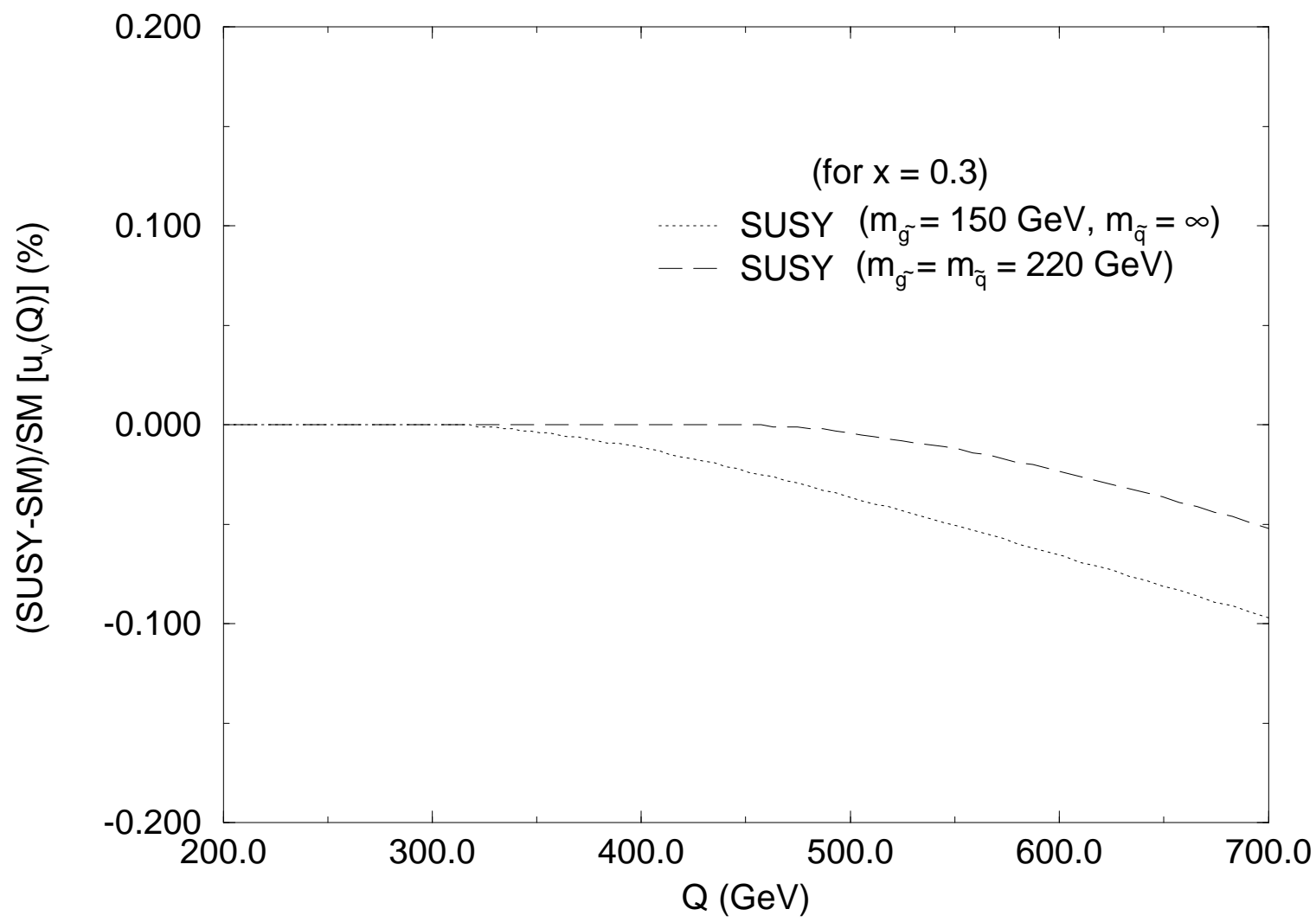


Fig. 2

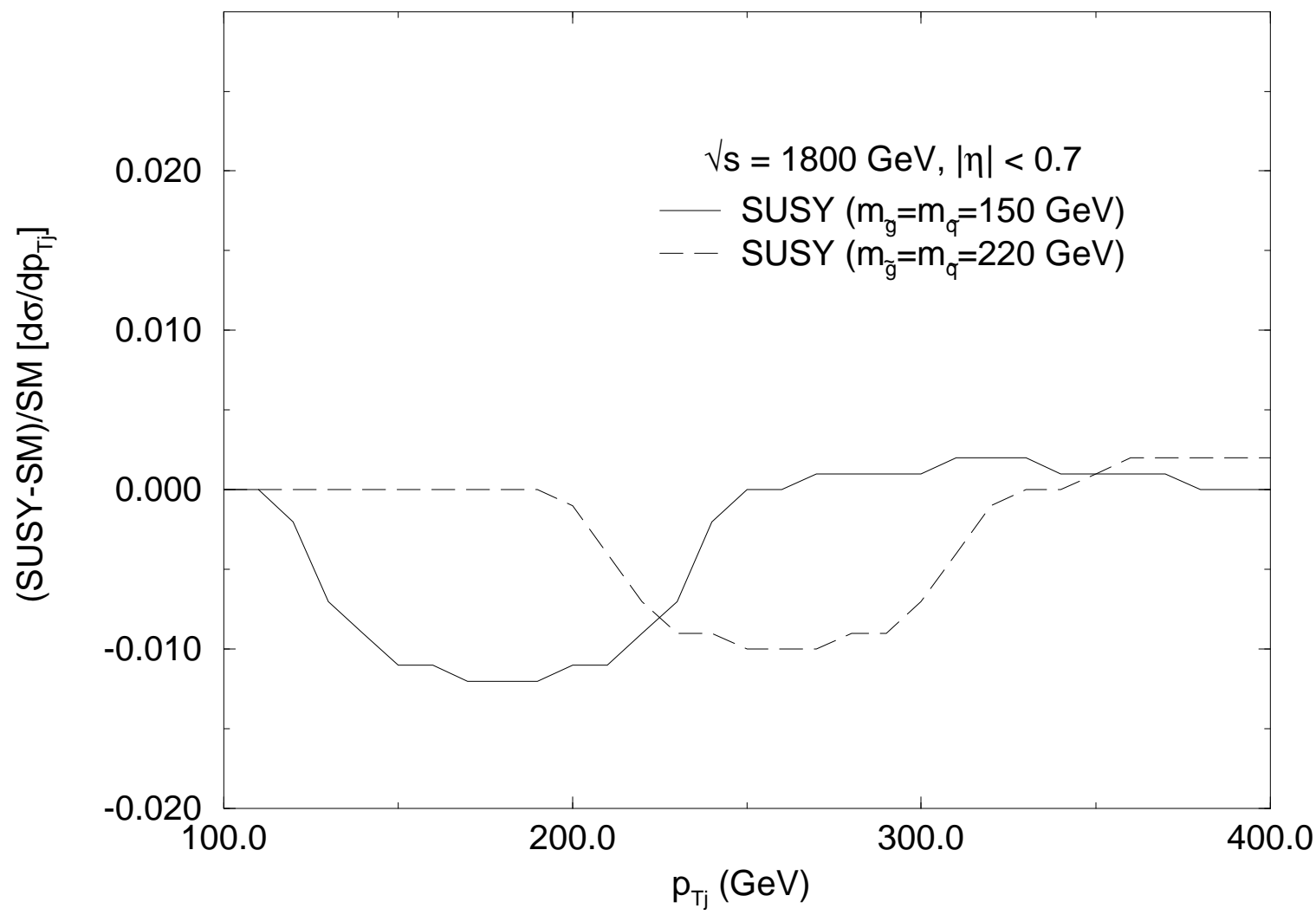


Fig. 3

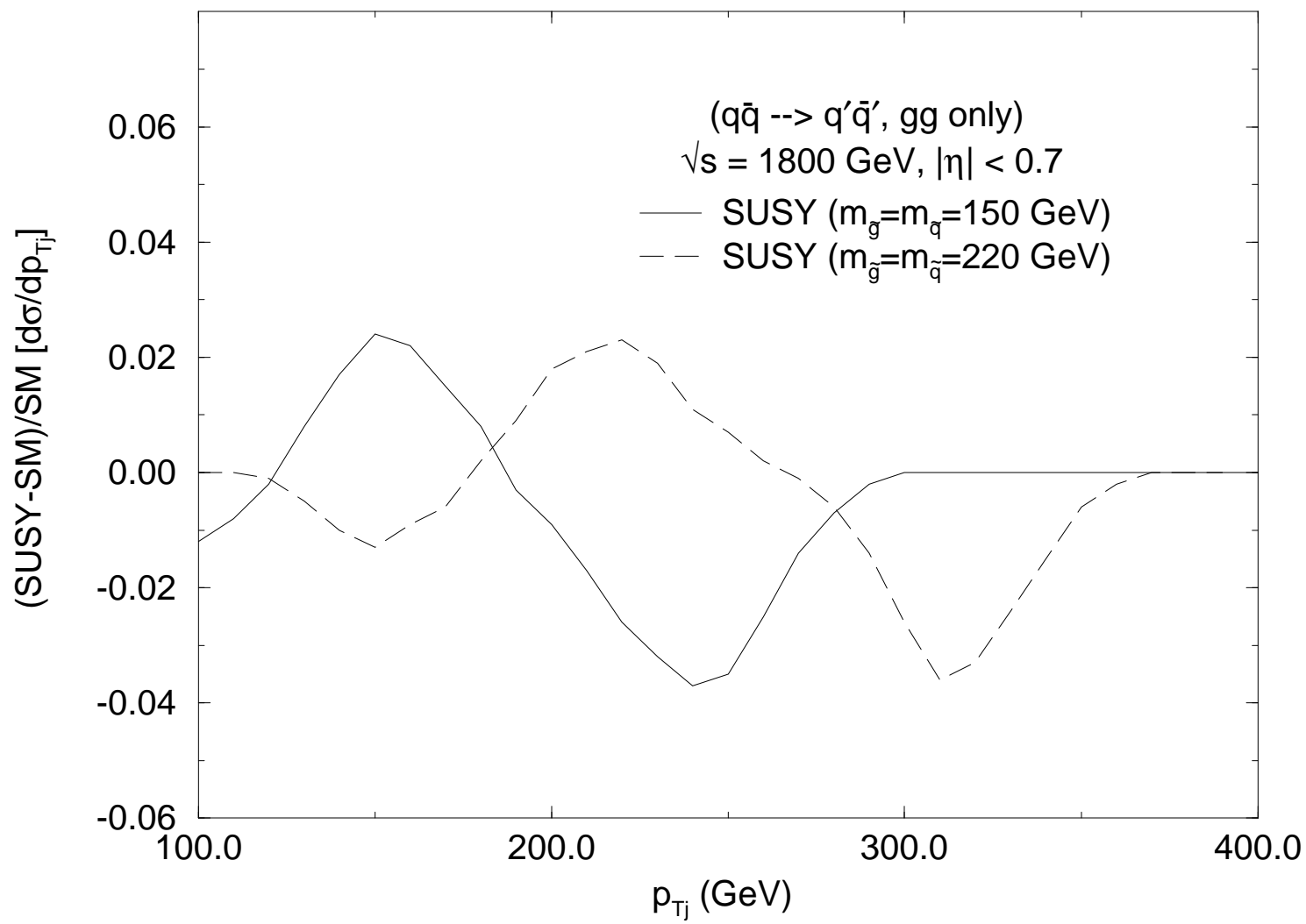


Fig. 4(a)

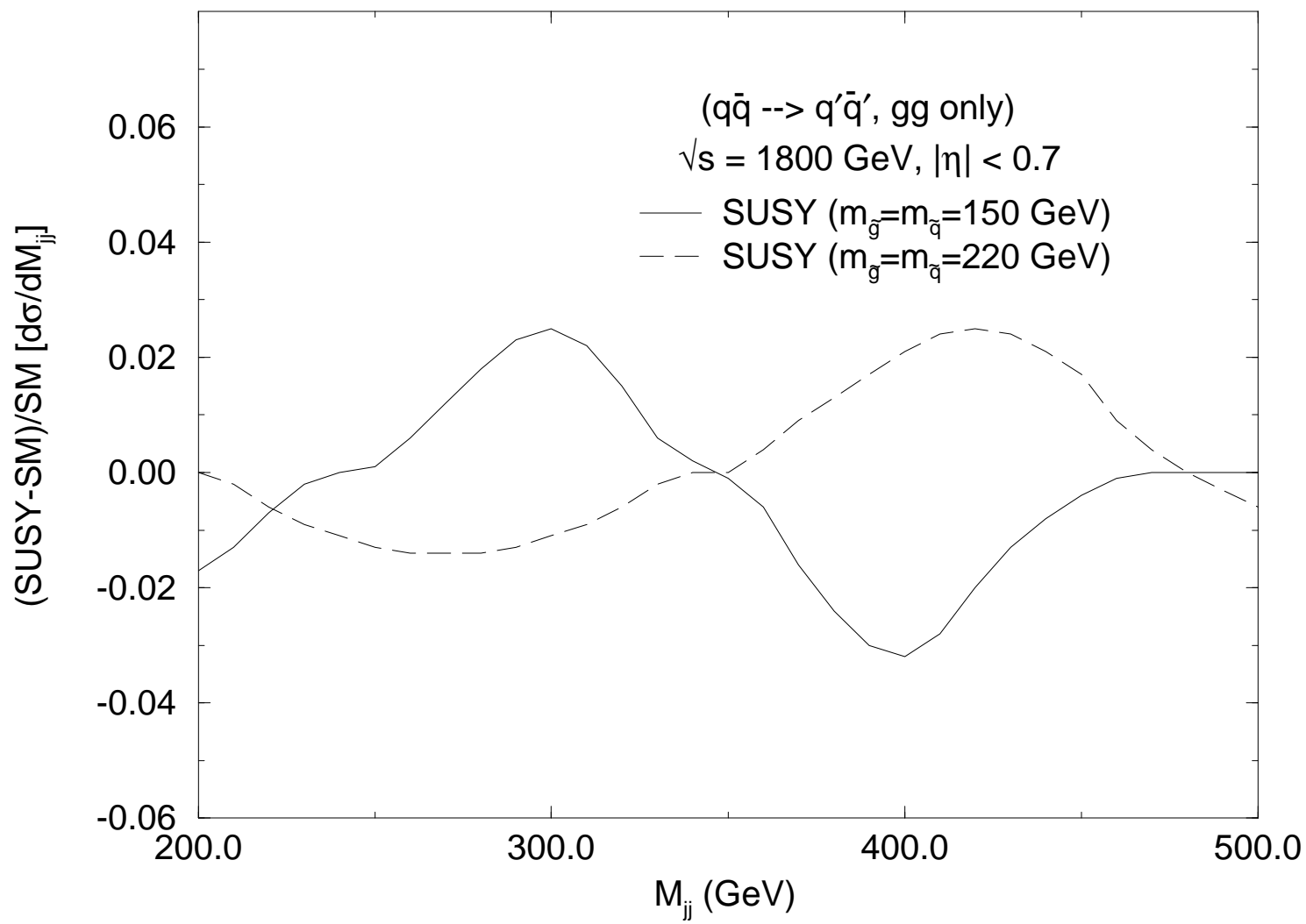


Fig. 4(b)